JOURNAL OF MATERIALS SCIENCE **39** (2004) 2927–2929

Cyclic stress response behavior of a carbide-strengthened Co-base alloy under low cycle fatigue at 900 °C

F. M. YANG*, X. F. SUN, H. R. GUAN, Z. Q. HU
Institute of Metals Research, Chinese Academy of Sciences, Shenyang 110016, People's Republic of China
E-mail: fuminyang@sohu.com

A carbide strengthened cobalt-base superalloy, K40S alloy, which exhibits an excellent combination of high temperature strength, tensile ductility and corrosion resistance is currently used for high temperature components in gas turbine engines [1]. Low cycle fatigue (LCF) at elevated temperature is an important consideration in the design of turbine components such as disks and turbine blades. There are two important aspects in the LCF research: development of a life-predication model and determination of the effect of the microstructural change. Both have been the subjects of many studies [2–9]. Phenomena keenly related to microstructural changes are cyclic hardening and cyclic softening. Among superalloys, cyclic hardening mechanisms have been principally attributed to the immobility of dislocations resulting from the multiplication of dislocations and their interactions or from the dislocation-precipitate interactions and dislocation-solute atmosphere interactions [10–12]. However, there appears to be no consensus on the cause of cyclic softening. Antolovich *et al*. [4] attributed the cyclic softening of RENÉ80 at 871 and 980 °C to the loss of coherency due to particle coarsening, in which micrographs of misfit dislocations were present as evidence. Rao *et al*. [13] reported that cyclic softening occurred in Inconel 617 at 850 °C under a strain rate lower than $4 \times 10^{-5}\,s^{-1}$. At higher strain rates, cyclic hardening was observed. The authors attributed cyclic softening to dislocation annihilation and rearrangement, and cyclic hardening to dynamic strain aging. Recent studies on a nickel-iron base superalloy [14, 15] have attributed the subsequent softening to a reduction in the size of γ' because of shearing by glide dislocations.

The purpose of this paper is to report some recent observations pertaining to the strain rate dependence of cyclic stress response and evolving deformation substructure of K40S cobalt-base superalloy at 900 °C. A detailed examination of the deformation substructure has been conducted with a view to understanding the features that may influence cyclic stress response.

The cyclic stress response behavior represents the locus of the peak tensile stress with successive cycles. The changes in peak tensile amplitude with the number of cycles at 900 °C are depicted in Fig. 1. The alloy exhibited an initial cyclic hardening followed by cyclic softening, which continued until the stress decreased rapidly due to the formation of microcracks and their subsequent growth.

The typical microstructure of K40S alloy constitutes a continuous γ-fcc Co matrix and the primary carbide M_7C_3 in intergranular and interdendritic regions [16] in the form of rods or irregular aggregates, forming a continuous network around the grained matrix. Carbide is the most important secondary phase in K40S alloy, and contributes significantly to alloy strengthening.

A substantial microstructural change has occurred in the specimens, even with the shortest fatigue life, $2N_f = 300$ cycles. Fig. 2 is a typical microstructure of the ruptured specimen. It can be seen that a profusion of secondary precipitates have been produced, and the secondary precipitates are unevenly distributed. Surrounding the primary carbide, M_7C_3, there is a dense distribution of fine precipitates. Transmission electron micrographs exhibit that the precipitates have a cuboidal morphology [17]. All these precipitates possess the same crystal structure and their characteristic reflections are present at every one third position of the fcc matrix reflections. This indicates that the precipitates have a structure with a lattice constant that is nearly three times that of the matrix, and they have a cube-cube orientation relationship with the matrix:

$$\{100\}_p // \{100\}_\gamma$$
$$\langle 100\rangle_p // \langle 100\rangle_\gamma$$

these are characteristic feature of the chromium-rich $M_{23}C_6$ carbide [18].

The LCF loading changed the substructure of K40S alloy significantly, the most pronounced change being an increase in the density of dislocation. As cobalt base superalloy, K40S alloy has low stacking-fault energy. Stacking-faults can be easily made active. Stacking-faults piled up and some were interrupted by secondary carbide particles (as shown in Fig. 3a marked by arrow). Two types of dislocation structures were identified: matrix dislocation and interfacial dislocation at the secondary carbide $M_{23}C_6/\gamma$ interphase boundary. Typical micrographs of each kind of dislocation structure are shown in Fig. 3. Matrix dislocations were highly concentrated around secondary carbides due to the secondary carbide pinning and dislocation-dislocation interactions (Fig. 3b). Interfacial dislocations (Fig. 3c)

*Author to whom all correspondence should be addressed.

0022–2461

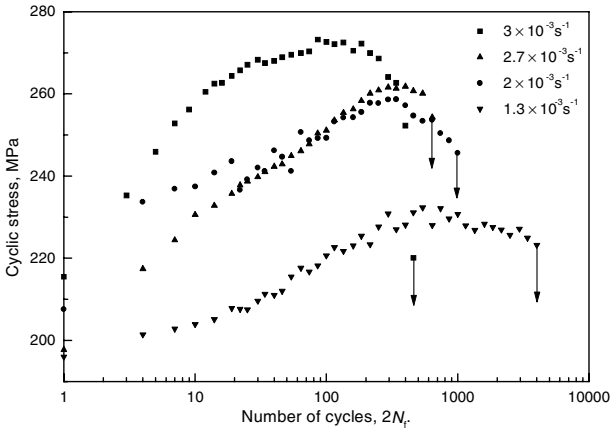

Figure 1 Cyclic stress response of K40S alloy as a function of strain rate at 900 °C.

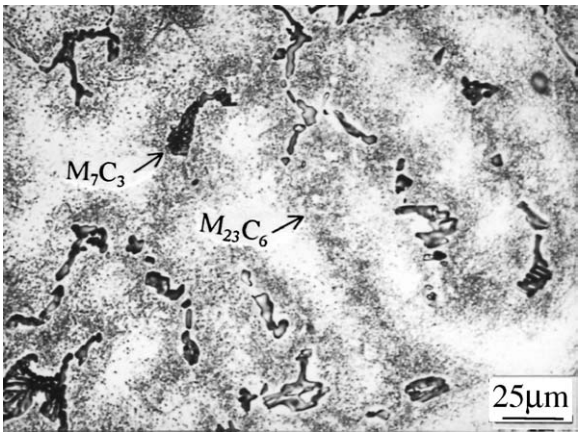

Figure 2 Secondary precipitates in a ruptured specimen ($\dot{\varepsilon} = 3 \times 10^{-3}$ s^{-1} and $2N_f = 300$).

accompanying coarsening of the secondary carbide particles were observed in specimens interrupted after the cyclic softening began.

The cyclic stress response behavior can be explained by the mechanisms associated with dislocation-dislocation interactions and dislocation-precipitate interactions [19, 20].

The stacking faults were cut by dislocations moving and interrupted by secondary carbides (Fig. 3a). Dislocations piled up and some were pinned at secondary carbide particles (Fig. 3b) which act as obstacle and hinder the motion of dislocations. It is an energy consuming process to make the locked dislocations move. In order to maintain the strain rate, the response stress has to increase enough to generate additional mobile dislocations or unlock the pinned dislocations, exhibiting initial cyclic hardening.

As shown in Fig. 1, K40S alloy exhibited cyclic hardening to a maximum stress followed by cyclic softening. The following softening stage was not due to crack nucleation, which generally occurred late in the fatigue life. For secondary carbide $M_{23}C_6$ has no coherency of γ matrix, present work indicates that the mechanism of cyclic softening of K40S alloy at 900 °C is different from what has been suggested except for particle coarsening reported by Antolovich [4]. No dislocation annihilation reported by Rao *et al.* [13] and the precipitates shearing reported by Valsan *et al.* [14,15] but

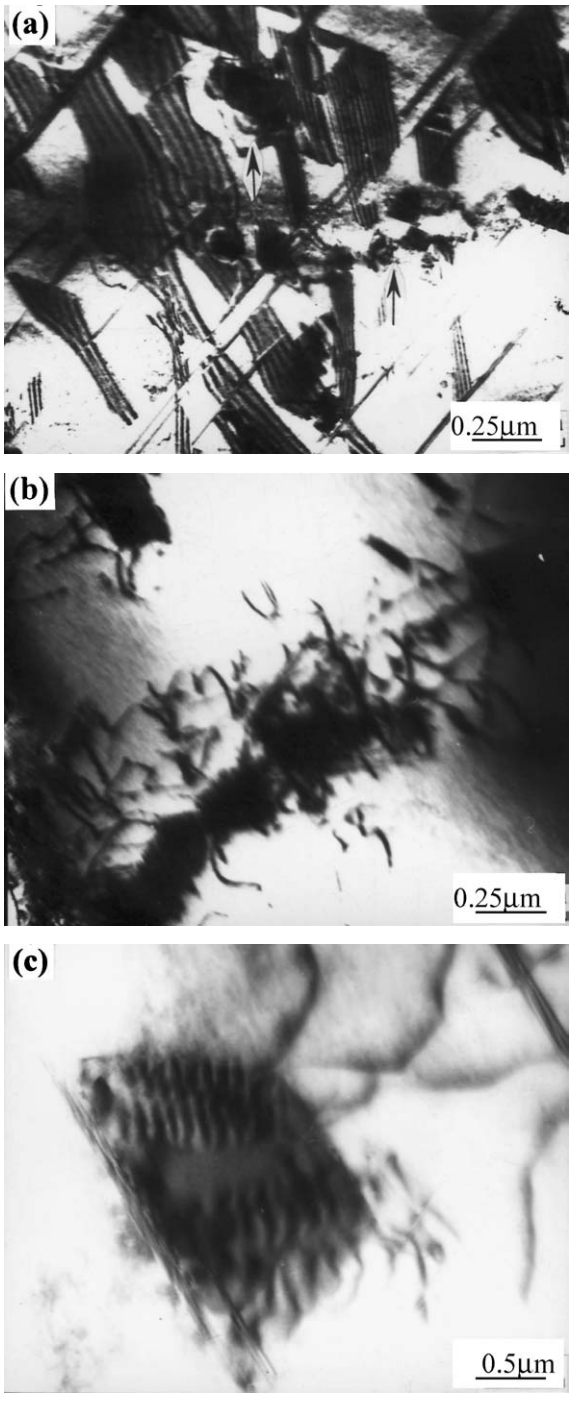

Figure 3 Typical TEM micrograph showing: (a) the stacking faults, (b) dislocation tangles and the dislocations pinned at secondary carbides and (c) misfit dislocations ($\dot{\varepsilon} = 2 \times 10^{-3}$ s^{-1}, $2N_f = 400$).

interfacial dislocations at the interphase boundary were observed in the course of cyclic softening. The interfacial dislocations, resulting from a stress due to secondary carbide $M_{23}C_6$ volume change may be a direct evidence for explaining the following cyclic softening behavior of K40S alloy.

References

1. F. M. YANG, X. F. SUN, H. R. GUAN and Z. Q. HU, *Metall. Trans.* **34A** (2003) 979.
2. G. EBI, H. RIEDEL and P. NEUMANN, "Fracture Control of Engineering Structures" (ECF6), edited by H. C. VanElst and A. Bakker (Kingdom, 1986) Vol. 3, p. 1587.
3. H. H. HEITMANN, H. VEHOFF and P. NEUMANN, Advances in Fracture Research 84, Proc. ICF6, edited by S. R. Valluri,

D. M. R. Taplin, P. R. Rao, J. F. Knott and R. Dubey (Pergamon Press Ltd., Oxford and New York, 1984) Vol. 5, p. 3599.
4. S. D. ANTOLOVICH, S. LIU and R. BAUR, *Metall. Trans.* **12A** (1981) 473.
5. R. V. MINER and M. G. CASTELLI, *ibid.* **23A** (1992) 551.
6. S. K. HWANG, *Scripta Metall.* **5** (1981) 35.
7. S. K. HWANG and C.S. PANDE, *Metall. Trans.* **14A** (1983) 2021.
8. H. F. MERRICK, *ibid.* **5A** (1974) 891.
9. D. FOURNIER and A. PINEAU, *ibid.* **8A** (1977) 1095.
10. M. VALSAN, D. H. SASTRY, K. B. S. RAO and S. L. MANNAN, *ibid.* **25A** (1994) 159.
11. K. B. S. RAO, M. G. CASTELLI, G. P. ALLEN and J. R. ELLIS, *ibid.* **28A** (1997) 347.
12. K. B. S. RAO, M. G. CASTELLI and J. R. ELLIS, *Scripta Metall.* **33** (1995) 1005.
13. K. B. S. RAO, H. SCHIFFERS, H. SCHUSTER and H. NICKEL, *Metall. Trans.* **19A** (1988) 359.
14. M. VALSAN, D. H. SASTRY, K. B. S. RAO and S. L. MANNAN, *ibid.* **25A** (1994) 159.
15. M. VALSAN, Ph.D. Thesis, Indian Institute of Science, Bangalore, India, 1991.
16. F. M. YANG, X. F. SUN, W. ZHANG, Y. P. KANG, H. R. GUAN and Z. Q. HU, *Mater. Lett.* **49** (2001) 160.
17. F. M. YANG, X. F. SUN, H. R. GUAN and Z. Q. HU, *Acta Metall. Sinica.* **38** (2002) 1047.
18. H. M. TAWANAY, *J. Mater. Sci.* **18** (1983) 2976.
19. K. B. S. RAO, H. SCHIFFERS and H. SCHUSTER, *Metall. Trans.* **19A** (1988) 359.
20. V. R. SRINIVASAN, R. SANDHYA, K. B. S. RAO, S. L. MANNAN and K. S. RAGHAVAN, *Int. J. Fatigue* **13** (1991) 471.

Received 8 October
and accepted 21 October 2003